X-ray Continuum Emission and Broad Iron Lines

Introduction

AGN have power law continua.

Purpose of this lecture: investigate physical origin of the continuum emission.

Structure:

1. Compton Scattering and Comptonization
2. Source of hot electrons
3. X-ray Reflection
4. Relativistic Broadened Fe Kα Lines

AGN X-Ray Continua

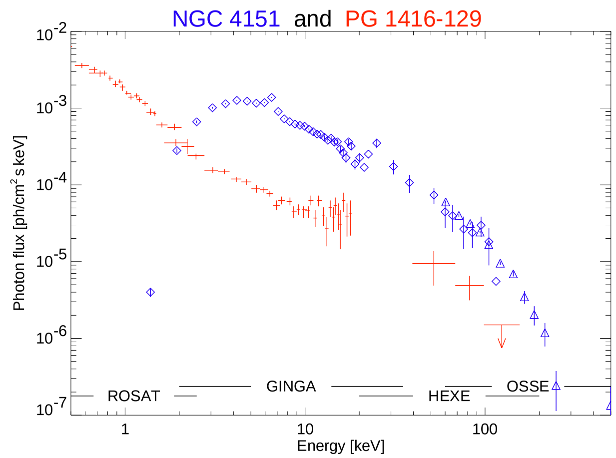

(PG 1416−129: de Kool et al., 1994, Williams et al., 1992, Staubert & Maisack, 1996; NGC 4151: Maisack 1991, 1993)

Note: NGC 4151 not corrected for interstellar absorption.

Spectral shape of AGN very similar to galactic Black Holes $\Longrightarrow$ Same physical mechanism (=Comptonization) responsible!

Thomson Scattering

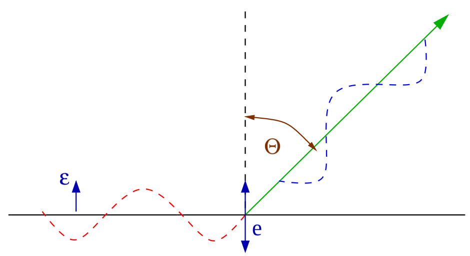

after Rybicki&Lightman, Fig. 3.6

Look at radiation from free electron in response to excitation of electron by an electromagnetic wave $E_0 \sin \omega_0 t$ (pointing in direction of unit-vector $\boldsymbol{\epsilon}$):

Force on charge

$$\mathbf{F} = m_e \dot{\mathbf{v}} = q E_0 \sin \omega_0 t \, \boldsymbol{\epsilon} \tag{3.1}$$

This neglects the B-field, i.e., assumes $v \ll c$.

$\Longrightarrow$ The electron feels an acceleration, $\dot{\mathbf{v}}$, and therefore it radiates!

Thomson Scattering

The power radiated by an accelerated charge in direction Θ through the spherical angle $d\Omega$ is given by Larmor's formula:

$$\frac{dP}{d\Omega}(\Theta) = \frac{1}{16\pi^2 c^3 \epsilon_0} q^2 \dot{v}^2 \sin^2\Theta \tag{3.2}$$

Integrating Eq. (3.2) over 4π sr gives

$$P = \frac{q^2 \dot{v}^2}{6\pi c^3 \epsilon_0} \tag{3.3}$$

For the case the charge is accelerated by an (sinusoidally varying) electric field $E(t)$ one finds after a longish calculation:

$$\frac{dP}{d\Omega} = \frac{q^4 E_0^2}{16\pi^2 m^2 c^3 \epsilon_0} \sin^2\Theta \quad \text{and} \quad P = \frac{q^4 E_0^2}{12\pi c^3 m^2 \epsilon_0} \tag{3.4}$$

Thomson Scattering

The incident flux on the electron (i.e., $c \times$ energy density for radiation) is

$$\langle \mathbf{S} \rangle = \frac{c\epsilon_0}{2} E_0^2 \tag{3.5}$$

Define the differential cross section for Thomson scattering, $d\sigma/d\Omega$, such that

$$\frac{dP}{d\Omega} = \langle \mathbf{S} \rangle \frac{d\sigma}{d\Omega} \iff \frac{q^4 E_0^2}{16\pi^2 m^2 c^3 \epsilon_0} \sin^2\Theta = \frac{c\epsilon_0^2}{2} E_0^2 \frac{d\sigma}{d\Omega} \tag{3.6}$$

such that

$$\left.\frac{d\sigma}{d\Omega}\right|_{\text{polarized}} = \frac{q^4}{8\pi^2 m^2 c^4 \epsilon_0^2} \sin^2\Theta = r_0^2 \sin^2\Theta \tag{3.7}$$

with the classical electron radius

$$r_0 = \frac{e^2}{4\pi m_e c^2 \epsilon_0} = 2.82 \times 10^{-15}\,\text{m} \tag{3.8}$$

Thomson Scattering

The differential cross section $d\sigma/d\Omega$ is the area presented by the electron to a photon that is going to get scattered in direction $d\Omega$.

The total cross section for Thomson scattering, σ_T, is then obtained from the differential cross section by integrating $d\sigma/d\Omega$ from Eq. (3.7) over all angles:

$$P = \int \langle S \rangle \frac{d\sigma}{d\Omega} d\Omega = \langle S \rangle \int \frac{d\sigma}{d\Omega} d\Omega =: \langle S \rangle\, \sigma_\mathrm{T} \tag{3.9}$$

Performing the integration yields

$$\sigma_\mathrm{T} = \frac{8\pi}{3} r_0^2 = \frac{e^4}{6\pi m_e^2 \epsilon_0^2 c^4} = 6.652 \times 10^{-25}\,\text{cm}^2 \tag{3.10}$$

σ_T is also called the Thomson cross section.

Thomson Scattering

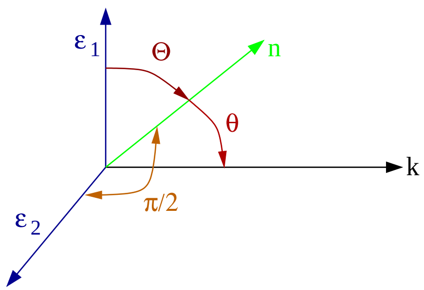

after Rybicki & Lightman, Fig. 3.7

For linear polarized light: scattered radiation is linearly polarized in the plane of incident polarization vector, $\boldsymbol{\epsilon}$, and direction of scattering, $\mathbf{n}$.

To compute σ for nonpolarized radiation, note:

nonpolarized radiation $= \sum$ polarized beams

at $\angle(90^\circ)$. Thus, to scatter nonpolarized radiation propagating in direction $\mathbf{k}$ into direction $\mathbf{n}$, need to average two scatterings:

$$\left.\frac{d\sigma}{d\Omega}\right|_{\text{unpol}} = \frac{1}{2}\left(\left.\frac{d\sigma(\Theta)}{d\Omega}\right|_{\text{pol}} + \left.\frac{d\sigma(\pi/2)}{d\Omega}\right|_{\text{pol}} \right) \tag{3.11}$$

Let $\theta = \angle(\mathbf{k}, \mathbf{n})$ to obtain

$$\left.\frac{d\sigma}{d\Omega}\right|_{\text{unpol}} = \frac{r_0^2}{2}(1+\cos^2\theta) = \frac{3\sigma_\mathrm{T}}{16\pi}(1+\cos^2\theta) \quad \text{and} \quad \int \frac{d\sigma}{d\Omega} d\Omega = \sigma_\mathrm{T} \tag{3.12}$$

Compton Scattering

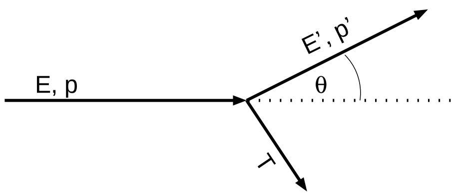

Thomson scattering: initial and final photon energy are identical.
But: in QM: light consists of photons
$\Longrightarrow$ Scattering: photon changes direction
$\Longrightarrow$ Momentum change
$\Longrightarrow$ Energy change!
This process is called Compton scattering.

Energy/wavelength change in scattering (see handout):

$$E' = \frac{E}{1 + \frac{E}{m_e c^2}(1 - \cos\theta)} \sim E\left(1 - \frac{E}{m_e c^2}(1 - \cos\theta)\right) \quad (3.13)$$

$$\lambda' - \lambda = \frac{h}{m_e c}(1 - \cos\theta) \quad (3.14)$$

where $h/m_e c = 2.426 \times 10^{-12}$ m (Compton wavelength).

Averaging over θ, for $E \ll m_e c$:

$$\frac{\Delta E}{E} \approx -\frac{E}{m_e c^2} \quad (3.15)$$

E.g., at 6.4 keV, $\Delta E \approx 0.2$ keV.

The derivation of Eq. (3.13) is most simply done in special relativity using four-vectors. In the following, we will use capital letters for four-vectors and small letters for three-vectors. Furthermore, we will adopt the convention

$$\mathbf{P}\cdot\mathbf{Q} = P_0Q_0 - P_1Q_1 - P_2Q_2 - P_3Q_3 \quad (3.16)$$

for the product of two four vectors, following, e.g., the convention of Rindler (1991, Introduction to Special Relativity).

The four-momentum of a particle with non-zero rest-mass, m_0, e.g., an electron, is

$$\mathbf{Q} = m_0\gamma\begin{pmatrix} c \\ \mathbf{v}\end{pmatrix} = \begin{pmatrix} m_0\gamma c \\ \mathbf{q}\end{pmatrix} \quad (3.17)$$

where $\mathbf{v}$ is the velocity of the particle and $\mathbf{q}$ its momentum. As usual, $\gamma = (1 - (v/c)^2)^{-1/2}$. The square of $\mathbf{Q}$ is

$$\mathbf{Q}^2 = m_0^2\gamma^2c^2 - m_0^2\gamma^2v^2 = m_0^2c^2\gamma^2\left(1 - \left(\frac{v^2}{c^2}\right)\right) = m_0^2c^2 \quad (3.18)$$

Obviously, $\mathbf{Q}^2$ is relativistically invariant.

In the same spirit, the four-momentum of a photon is

$$\mathbf{P} = \frac{E}{c}\begin{pmatrix} 1 \\ \hat{\mathbf{u}}\end{pmatrix} \quad (3.19)$$

where $\hat{\mathbf{u}}$ is an unit-vector pointing into the direction of motion of the photon. Note that for photons

$$\mathbf{P}^2 = 0 \quad (3.20)$$

as the photon's rest-mass is zero.

We will now look at the collision between a photon and an electron. We will denote the four-momenta after the collision with primed quantities.

Conservation of four-momentum requires

$$\mathbf{P} + \mathbf{Q} = \mathbf{P}' + \mathbf{Q}' \quad (3.21)$$

We now use a trick from Lightman et al. (1975, Problem Book in Relativity and Gravitation), solving this equation for $\mathbf{Q}'$ and squaring the resulting expression:

$$(\mathbf{P} + \mathbf{Q} - \mathbf{P}')^2 = (\mathbf{Q}')^2 \quad (3.22)$$

Since the collision is elastic, i.e., the rest mass of the electron is not changed by the collision,

$$\mathbf{Q}^2 = (\mathbf{Q}')^2 \quad (3.23)$$

furthermore, $\mathbf{P}^2 = (\mathbf{P}')^2 = 0$, such that

$$\mathbf{P}\cdot\mathbf{Q} - \mathbf{P}\cdot\mathbf{P}' - \mathbf{Q}\cdot\mathbf{P}' = 0 \quad\Longleftrightarrow\quad \mathbf{P}\cdot\mathbf{P}' = \mathbf{Q}\cdot(\mathbf{P} - \mathbf{P}') \quad (3.24)$$

But in the frame where the electron is initially at rest,

$$\mathbf{Q}\cdot(\mathbf{P} - \mathbf{P}') = m_e c\left(\frac{E}{c} - \frac{E'}{c}\right) = m(E - E') \quad (3.25)$$

$$\mathbf{P}\cdot\mathbf{P}' = \frac{E}{c}\frac{E'}{c}(1 - \hat{\mathbf{u}}\cdot\hat{\mathbf{u}}') = \frac{EE'}{c^2}(1 - \cos\theta) \quad (3.26)$$

where $\theta = \angle(\hat{\mathbf{u}}, \hat{\mathbf{u}}')$. Inserting into Eq. (3.24) and solving for E' gives Eq. (3.13).

Compton Scattering

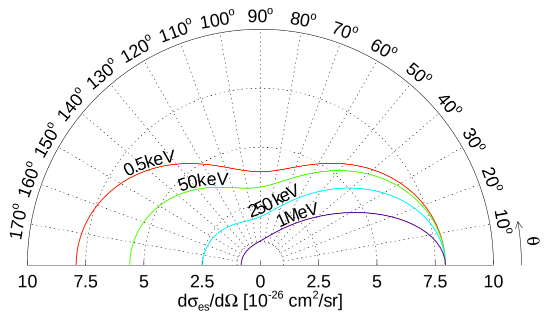

The proper derivation of cross section is done in quantum electrodynamics.
In the limit of low energies: will find Thomson result, for higher energies: relativistic effects become important.

For unpolarized radiation,

$$\frac{d\sigma_{es}}{d\Omega} = \frac{3}{16\pi}\sigma_T\left(\frac{E'}{E}\right)^2\left(\frac{E}{E'} + \frac{E'}{E} - \sin^2\theta\right) \quad (3.27)$$

(Klein-Nishina formula).

Compton Scattering

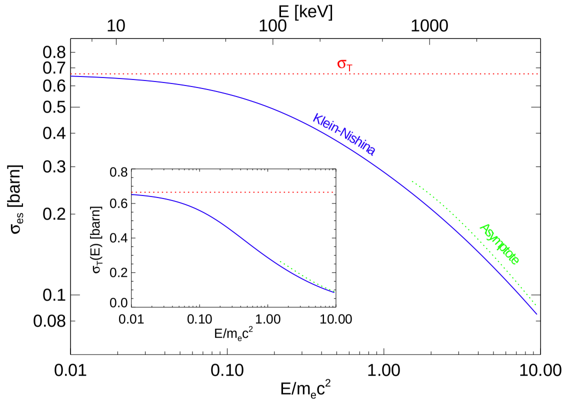

1 barn $= 10^{-28}$ m^2

Integrating over $d\sigma_{\text{es}}/d\Omega$ gives total cross-section:

$$\sigma_{\text{es}} = \frac{3}{4}\sigma_{\text{T}}\left[\frac{1+x}{x^3}\left\{\frac{2x(1+x)}{1+2x} - \ln(1+2x)\right\} + \frac{1}{2x}\ln(1+2x) - \frac{1+3x}{(1+2x)^2}\right] \quad (3.28)$$

where $x = E/m_{\text{e}}c^2$.

Energy Exchange

For non-stationary electrons, use previous formulae and Lorentz transform photon into electron's frame of rest (FoR):

1. Lab system ⇒ electron's frame of rest:

$$E_{\text{FoR}} = E_{\text{Lab}}\gamma(1 - \beta\cos\theta) \quad (3.29)$$

2. Scattering occurs, gives E'_{FoR}.
3. Electron's frame of rest ⇒ Lab system:

$$E'_{\text{Lab}} = E'_{\text{FoR}}\gamma(1 + \beta\cos\theta') \quad (3.30)$$

Therefore, if electron is relativistic:

$$E'_{\text{Lab}} \sim \gamma^2 E_{\text{Lab}} \quad (3.31)$$

since (on average) θ, θ' are $\mathcal{O}(\pi/2)$ (beaming!).

Thus: Energy transfer is *very* efficient.

As shown in the following, in Compton scattering the radiation field is also amplified by a factor γ^2.

We first look at the energy budget of one single scattering.

The total power *emitted* in the frame of rest of the electron is given by

$$\left.\frac{dE'_{\text{FoR}}}{dt_{\text{FoR}}}\right|_{\text{em}} = \int c\sigma_{\text{T}}E'_{\text{FoR}}V'(E'_{\text{FoR}})dE'_{\text{FoR}} \quad (3.32)$$

where $V'(E')$ is the photon energy density distribution (number of photons per cubic metre with an energy between E' and $E' + dE'$).

This power is Lorentz invariant:

$$\frac{V_{\text{Lab}}(E_{\text{Lab}})dE_{\text{Lab}}}{E_{\text{Lab}}} = \frac{V_{\text{FoR}}(E_{\text{FoR}})dE_{\text{FoR}}}{E_{\text{FoR}}} \quad (3.33)$$

In the "Thomson limit" one assumes that the energy change of the photon in the rest frame of the electron is small,

$$E'_{\text{FoR}} = E_{\text{FoR}} \quad (3.34)$$

(this limit was also used in the derivation of Eq. (3.31)). Furthermore one can show that the power is Lorentz invariant:

$$\frac{dE_{\text{FoR}}}{dt_{\text{FoR}}} = \frac{dE_{\text{Lab}}}{dt_{\text{Lab}}} \quad (3.35)$$

(this follows from the fact that energy and time are both "time-like quantities", i.e., the formulae for the Lorentz transform of energy and time are the same).

Therefore

$$\left.\frac{dE_{\text{Lab}}}{dt_{\text{Lab}}}\right|_{\text{em}} = c\sigma_{\text{T}}\int E^2_{\text{FoR}}\frac{V_{\text{FoR}}dE_{\text{FoR}}}{E_{\text{FoR}}} \quad (3.36)$$

$$= c\sigma_{\text{T}}\int E^2_{\text{FoR}}\frac{V_{\text{Lab}}dE_{\text{Lab}}}{E_{\text{Lab}}} \quad (3.37)$$

…Lorentz transforming E_{FoR}

$$= c\sigma_{\text{T}}\gamma^2\int(1-\beta\cos\theta)^2E_{\text{Lab}}V_{\text{Lab}}dE_{\text{Lab}} \quad (3.38)$$

…averaging over angles ($\langle\cos\theta\rangle = 0$, $\langle\cos^2\theta\rangle = \frac{1}{3}$)

$$= c\sigma_{\text{T}}\gamma^2\left(1+\frac{\beta^2}{3}\right)U_{\text{rad}} \quad (3.39)$$

where

$$U_{\text{rad}} = \int EV(E)dE \quad (3.40)$$

(initial photon energy density).

To determine the power gain of the photons, we need to subtract the power irradiated onto the electron,

$$\left.\frac{dE_{\text{Lab}}}{dt_{\text{Lab}}}\right|_{\text{inc}} = c\sigma_{\text{T}}\int EV(E)dE = \sigma_{\text{T}}cU_{\text{rad}} \quad (3.41)$$

Therefore, since

$$\gamma^2 - 1 = \gamma^2\beta^2 \quad (3.42)$$

the net power gain of the photon field is

$$P_{\text{compt}} = \left.\frac{dE_{\text{Lab}}}{dt}\right|_{\text{em}} - \left.\frac{dE_{\text{Lab}}}{dt}\right|_{\text{inc}} \quad (3.43)$$

$$= \frac{4}{3}\sigma_{\text{T}}c\gamma^2\beta^2U_{\text{rad}} \quad (3.44)$$

Amplification factor

As shown before, in the electron frame of rest,

$$\frac{\Delta E}{E} = -\frac{E}{m_e c^2} \tag{3.15}$$

Assuming a thermal (Maxwell) distribution of electrons (i.e., they're not at rest), using the equations from the previous slides one can show that the relative energy change is given by

$$\frac{\Delta E}{E} = \frac{4kT - E}{m_e c^2} = A \tag{3.45}$$

where A is the Compton amplification factor.

Thus:

$E \lesssim 4kT_e \Longrightarrow$ Photons gain energy, gas cools down.
$E \gtrsim 4kT_e \Longrightarrow$ Photons loose energy, gas heats up.

Amplification factor

In reality, photons will scatter more than once before leaving the hot electron medium.

The *total* relative energy change of photons by traversal of a hot ($E \ll kT_e$) medium with electron density n_e and size ℓ is then approximately

$$\left(\text{rel. energy change } y\right) = \frac{\text{rel. energy change}}{\text{scattering}} \times \left(\text{\# scatterings}\right) \tag{3.46}$$

The number of scatterings is $\max(\tau_e, \tau_e^2)$, where $\tau_e = n_e \sigma_T \ell$ ("optical depth"), such that

$$y = \frac{4kT_e}{m_e c^2} \max(\tau_e, \tau_e^2) \tag{3.47}$$

"Compton y-Parameter"

Spectral shape

Photon spectra can be found by analytically solving the "Kompaneets equation", but this is very difficult.

Approximate spectral shape from the following arguments:

After k scatterings, the energy of a photon with initial energy E_i is approximately

$$E_k = E_i A^k \tag{3.48}$$

But the probability to undergo k scatterings in a cloud with optical depth τ_e is $p_k(\tau_e) = \tau_e^k$ (follows from theory of random walks, note that the mean free path is $\ell = 1/\tau_e$).

Therefore, if there are $N(E_i)$ photons initially, then the number of photons emerging at energy E_k is

$$N(E_k) \sim N(E_i)(1 + A)^k \sim N(E_i)\left(\frac{E_k}{E_i}\right)^{-\alpha} \quad \text{with} \quad \alpha = -\frac{\ln \tau_e}{\ln A} \tag{3.49}$$

Comptonization produces power-law spectra.

General solution: Possible via the Monte Carlo method.

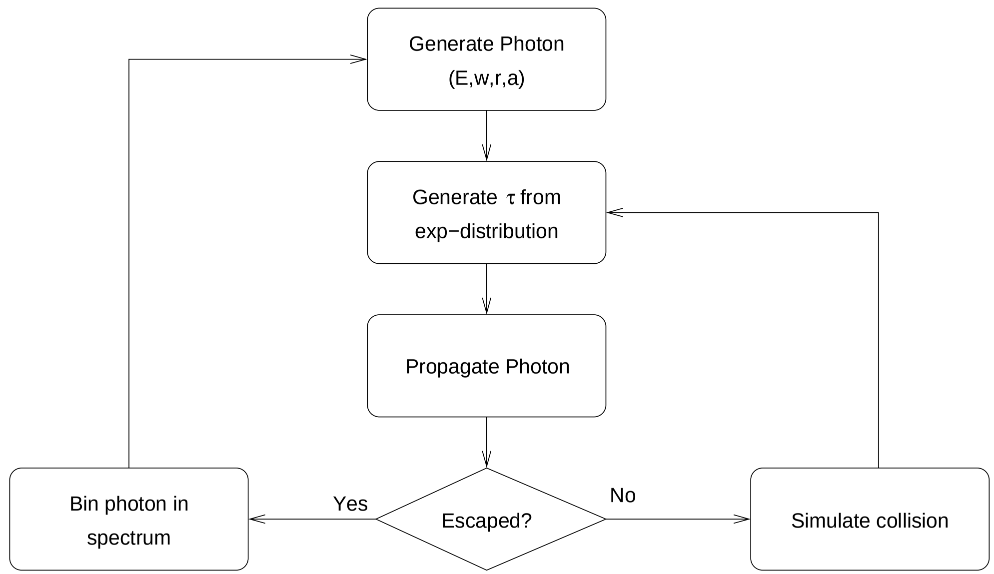

Spectral shape

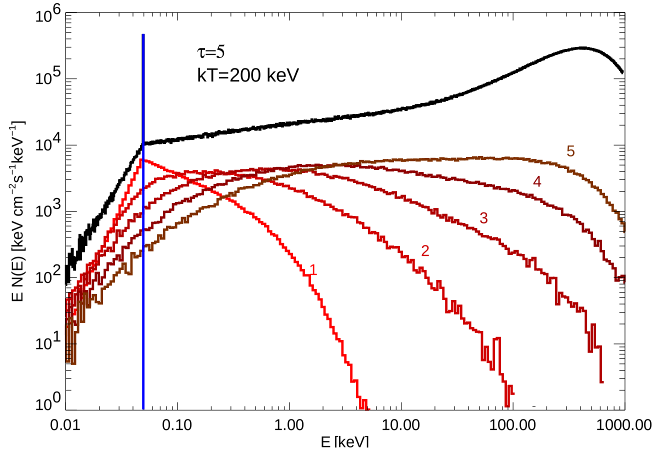

Monte Carlo simulation shows: Spectrum is $\Longrightarrow$ Power law with exponential cut-off (here: with additional "Wien hump", see next slide)

Spectral shape

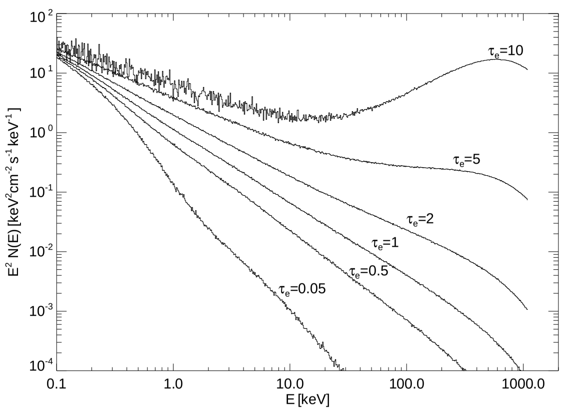

Sphere with $kT_e = 0.7 m_e c^2$ ($\sim$ 360 keV), seed photons come from center of sphere.

$y \ll 1$: pure power-law.
$y < 1$: power-law with exponential cut-off
$y \gg 1$: "Saturated Comptonization".

Saturated Comptonization has never been observed.

Galactic Black Holes

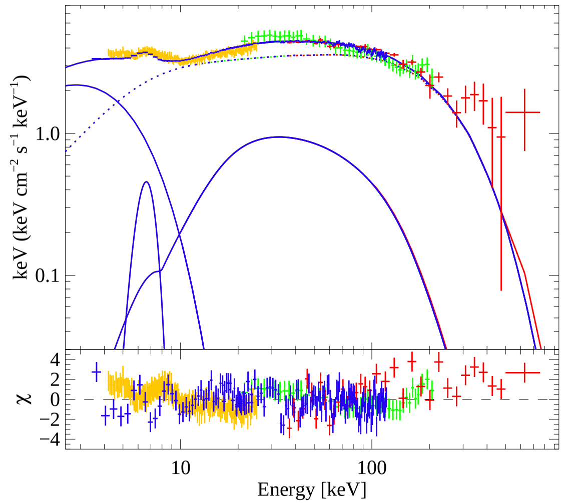

Fritz, et al., 2006

Fit of a *Comptonization* model to *RXTE/INTEGRAL* data from the galactic black hole Cygnus X-1.

$kT_{\text{soft}} = 1.21$ keV,
$\tau_e = 1.09$,
$kT_e \sim 100$ keV

Model works extremely well $\Longrightarrow$ Comptonization seems to explain the data.

Note the presence of a Compton reflection hump (evidence of close vicinity of hot electrons and only mildly ionized material)

Kα Line Diagnostics

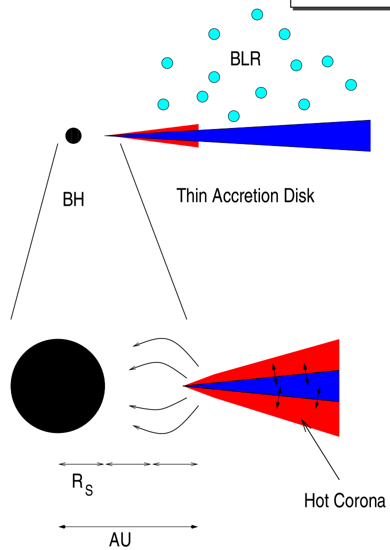

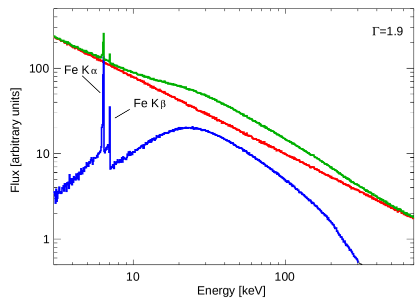

AGN X-Ray Spectrum:

- Comptonization of soft X-rays from accretion disk in hot corona ($T \sim 10^8$ K): power law continuum.
- Thomson scattering of power law photons in disk: Compton Reflection Hump
- Photoabsorption of power law photons in disk: fluorescent Fe Kα Line at $\sim$6.4 keV

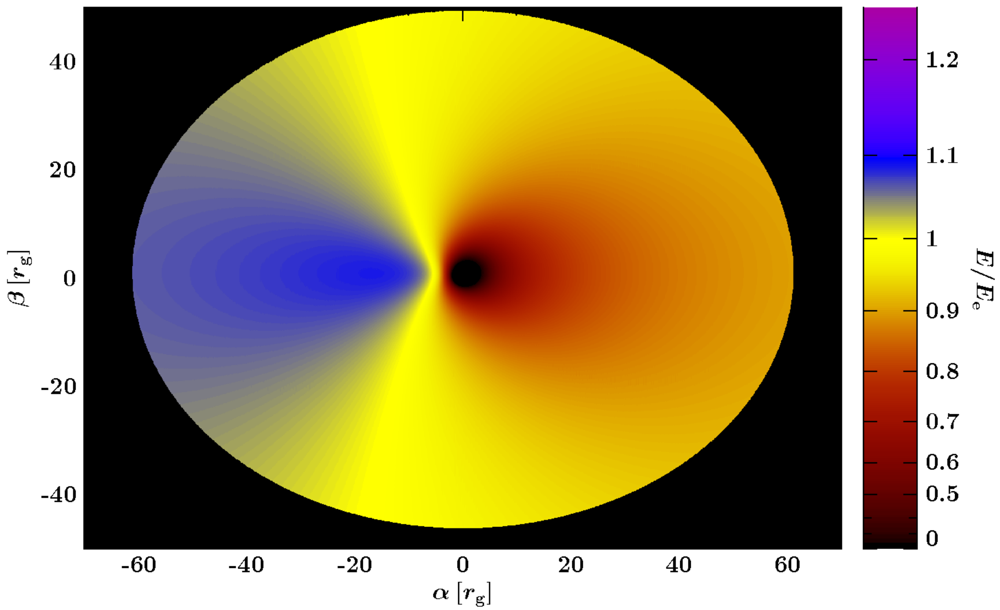

Kα Line Diagnostics

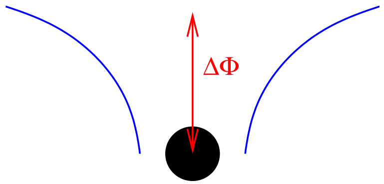

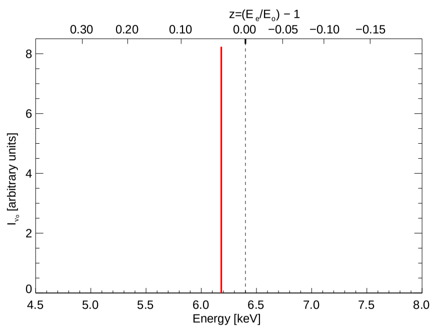

Total observed line profile affected by

- grav. Redshift

Kα Line Diagnostics

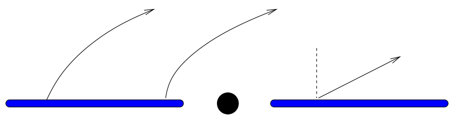

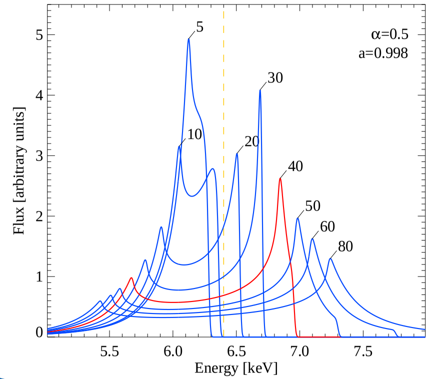

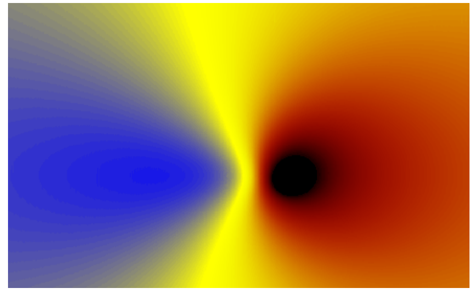

Total observed line profile affected by

- grav. Redshift
- Light bending
- rel. Doppler shift

Kα Line Diagnostics

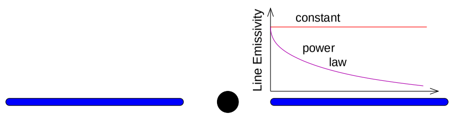

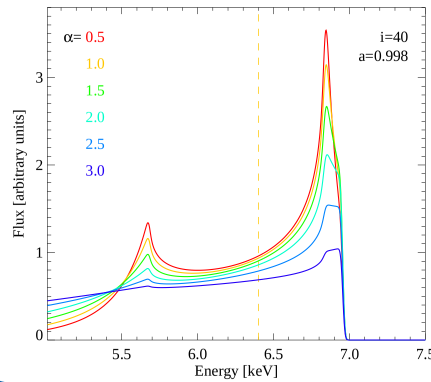

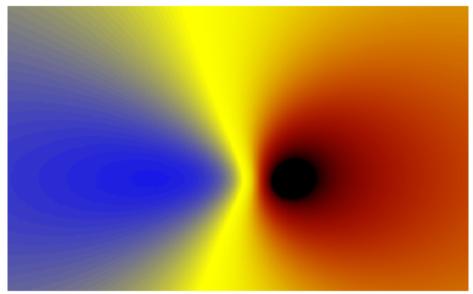

Total observed line profile affected by

- grav. Redshift
- Light bending
- rel. Doppler shift
- emissivity profile

Kα Line Diagnostics

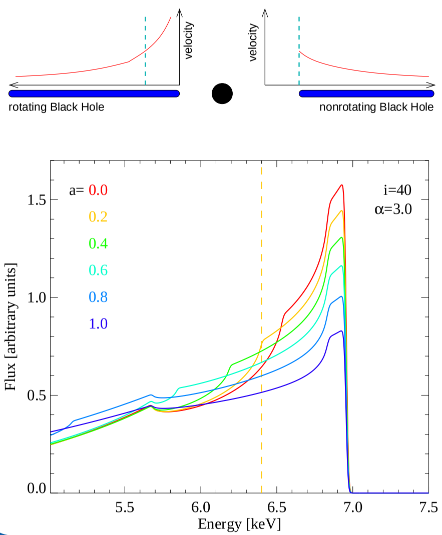

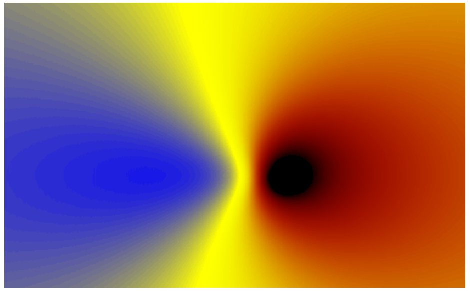

Total observed line profile affected by

- grav. Redshift
- Light bending
- rel. Doppler shift
- emissivity profile
- spin of black hole

MCG−6-30-15

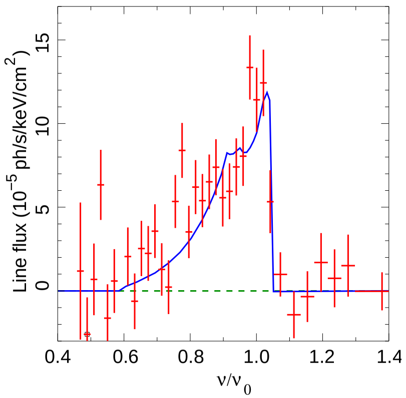

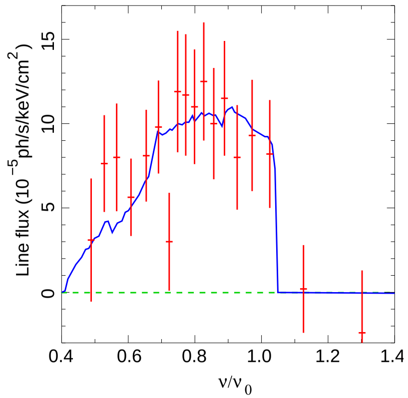

MCG−6-30-15 ($z = 0.008$): first AGN with relativistic disk line

Tanaka et al. (1995): time averaged *ASCA* spectrum: line skew symmetric
⟹ Schwarzschild black hole.

Iwasawa et al. (1996): "deep minimum state": extremely broad line
⟹ Kerr Black Hole.

Later confirmed with *BeppoSAX* (Guainazzi et al., 1999) and *RXTE* (Lee et al., 1999).

Broad Lines with ASCA

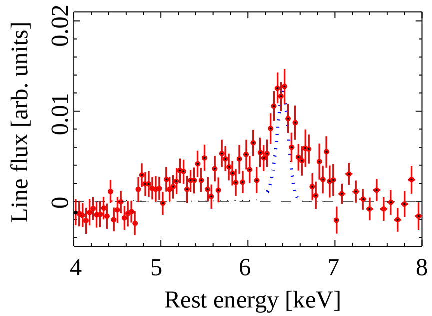

(Nandra et al., 1997, Fig. 4b)

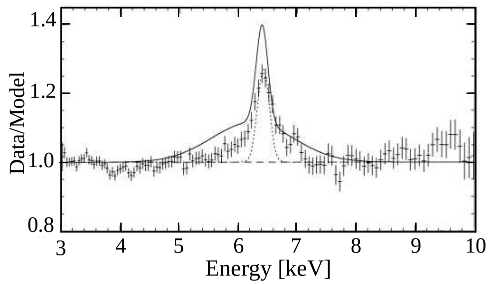

(Lubiński & Zdziarski, 2001, Fig. 2a)

ASCA: Average Seyfert Fe Kα profile contains a narrow core and a red and blue wings, but they are much weaker than MCG−6-30-15.

Best case: MCG−6-30-15

MCG−6-30-15

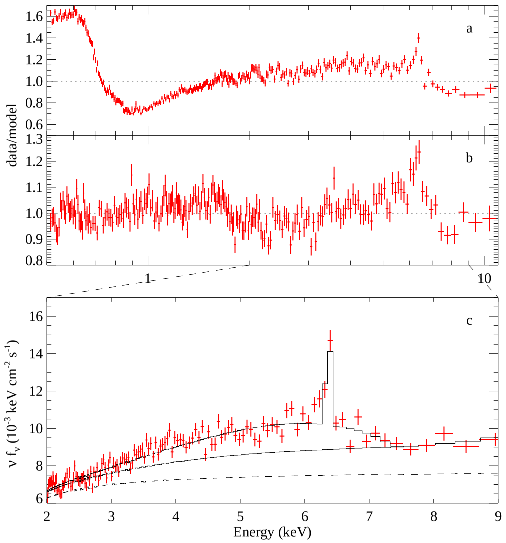

pure PL fit

Better modeling of soft excess and reflection $\Longrightarrow$ Fe Kα line has extreme width and skewed profile.

Components of the final fit.
$\Longrightarrow$ Line emissivity is strongly concentrated towards the inner edge of the disk ($\epsilon \propto r^{-4.6}$; cannot be explained with standard α-disk)

(*XMM-Newton*, June 2000, 100 ksec; Wilms et al., 2001)

MCG−6-30-15

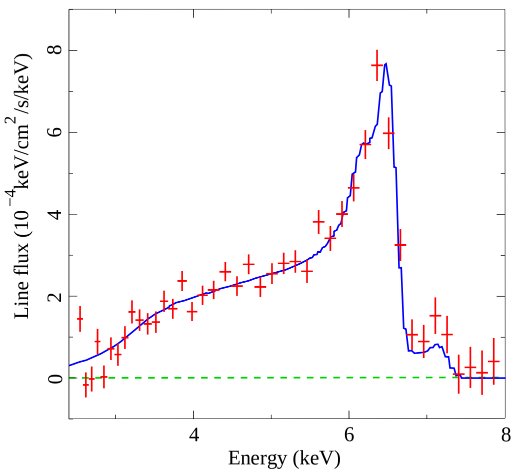

Fabian et al. (2002)

2001 July/August: 315 ksec observation (Fabian et al., 2002)

- Strong narrow line
- broad line clearly present
- emissivity profile very steep for radii close to r_{in}

  $I_{\text{Fe K}\alpha} \propto r^{-5.5\pm0.3}$ for $r < 6.1^{+0.8}_{-0.5} r_{\text{g}}$, $\propto r^{-2.7\pm0.1}$ outside that;
  Fabian & Vaughan (2003); confirms Wilms et al. (2001)

MCG−6-30-15

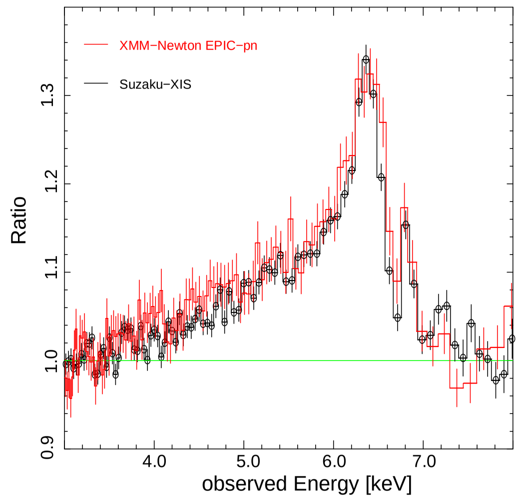

Suzaku (2006 Jan; ∼350 ksec; Miniutti et al., 2007)

Brenneman & Reynolds (2006): Angular momentum of BH in MGC−6-30-15 : $a = 0.989^{+0.009}_{-0.002}$.

Assuming no emission from within innermost stable circular orbit, (too) tightly constrained geometry.

Other Sources

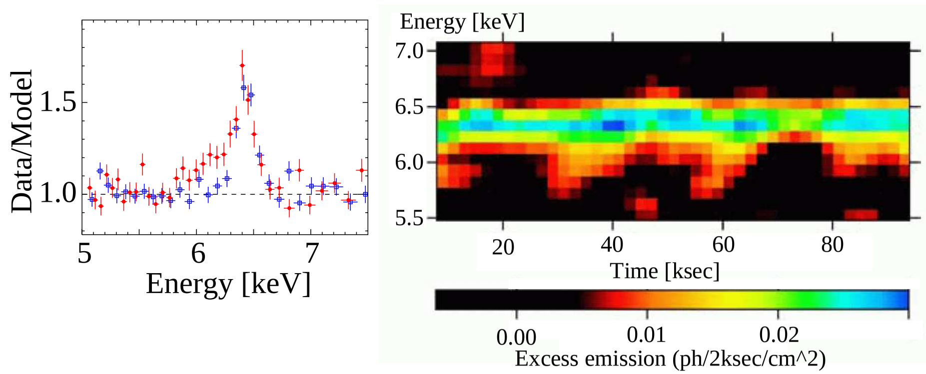

(Iwasawa, Miniutti & Fabian, 2004, Figs. 3,4)

Line profile variability in NGC 3516 $\Longrightarrow$ Corotating flare? ($7r_{\text{g}} \lesssim r \lesssim 16r_{\text{g}}$)

If interpretation is pushed further, gives $M \sim (1\ldots5)\times10^7\,M_\odot$.

Other Sources

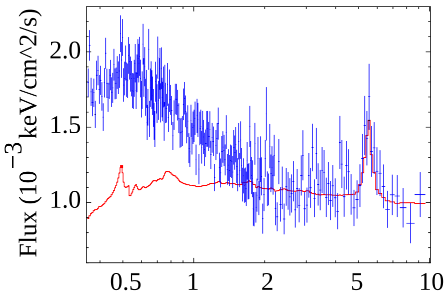

(Porquet & Reeves, 2003, Fig. 3)
XMM data from 2001

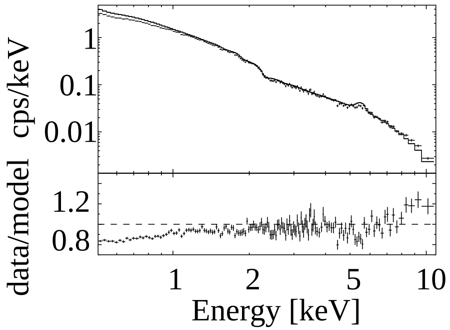

(Matt et al., 2005, Fig. 1)
comparison 2003 vs. 2001 data

Q0056−363 (broad line radio-quiet quasar, $L_X > 10^{45}\,\mathrm{erg\,s^{-1}}$):
Fe Kα has FWHM 24500 km s^{-1}, EW 275 eV

Q0056−363 is highest luminosity radio-quiet QSO with broad Fe Kα line.

Absorption or Lines?

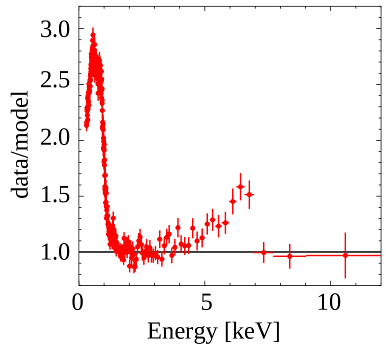

(1H0707−495; Fabian et al., 2004)

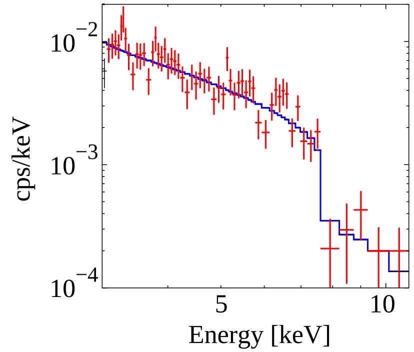

(IRAS 13224−3809; Boller et al., 2003)

NLSy1: Strong absorption or a relativistic line from a reflection dominated spectrum both describe the data equally well!

Similar results have been found by Pounds et al. in a variety of sources…

But: strong absorption models contradict observations where data >10 keV available, also Fe Lα line broadened (Fabian et al., 2009).

Other Sources

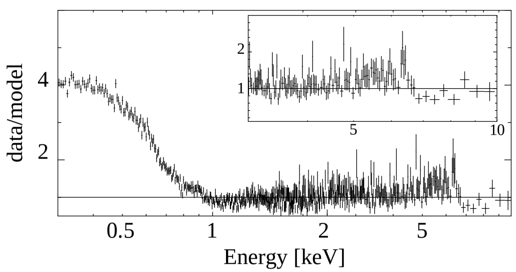

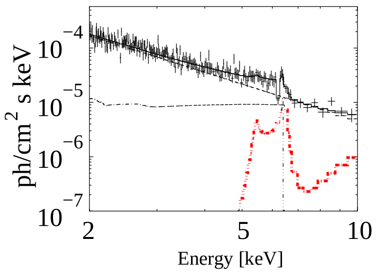

(Longinotti et al., 2003)

IRAS 13349+2436:

- Model either 2 broad emission lines *or*
- relativistic line from Fe XXIII/XXIV plus narrow absorption feature

Line shape can be rather complex!

Other examples include *blue*shifted lines, e.g., in Mkn 205 (Reeves et al., 2001) or Mkn 766.

Narrow Lines

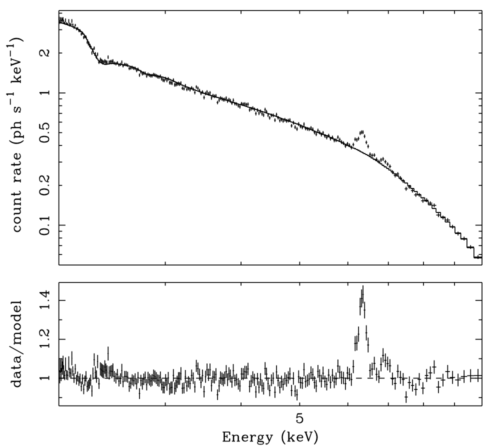

(NGC 4258; Reynolds et al. 2004)

The majority of Seyfert galaxies and QSOs do *not* show evidence for broad Fe Kα lines!

Narrow Lines

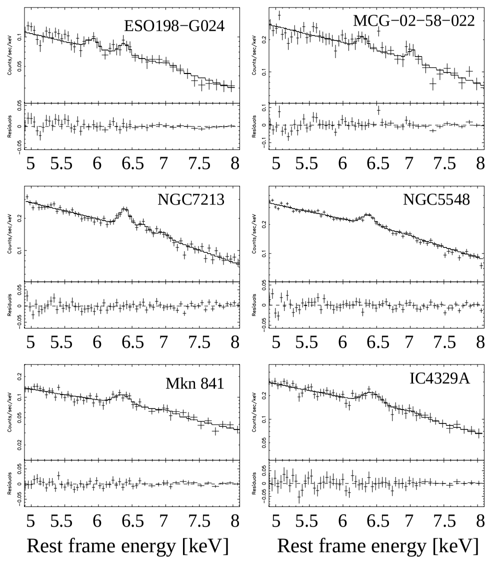

The majority of Seyfert galaxies and QSOs do *not* show evidence for broad Fe Kα lines!

statistics for PG-QSO: 20/38 show Fe Kα line, of these 3 have broad line (Jiménez-Bailón et al., 2005)

Bianchi et al. (2004, Fig. 4)
[Sample of Seyferts with simultaneous *BeppoSAX* observations.]

Conclusions

Relativistically broadened Fe Kα lines clearly do exist in a variety of different AGN

We need to rethink the details of the accretion process and the accretion geometry close to black hole:

- Energy extraction for extremely broad lines?
  Coupling BH – disk, structure of the inner disk (no torque condition?, structure of the infall region,...)

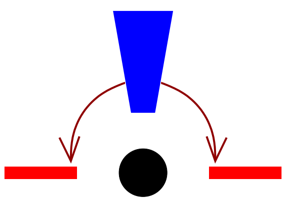

- "Lamppost model"?
  (Petrucci & Henri, 1997; Martocchia, Matt & Karas, 2002; Miniutti & Fabian, 2004)
  $\Longrightarrow$ X-rays focused down from the jet base?
  $\Longrightarrow$ If true, is continuum Comptonization?
  Fender et al. (2004), Markoff, Nowak & Wilms (2005) for galactic BHs

Conclusions

To be successful, models will have to consider:

- Broad Fe Kα lines are rare:
  - Truncated Disks?
  - Disk ionization (but needs fine tuning!)
  - And what about the Unified Model?
    Is the viewing angle really edge on?
- Narrow lines are ubiquitous:
  - Are they formed in the torus?
    but narrow lines often have FWHM$\sim$4000–7000 km s^{-1}
    $\Longrightarrow$ too large for torus! (expect $\sim$ 760 km s$^{-1}(M_8/r_{\rm pc})^{1/2}$)
  - Do they originate in the BLR or an ionized disk?

...and we should not forget the observational constraints: Strong Fe Kα variability $\Longrightarrow$ we need a larger collecting area (IXO!)

The Future

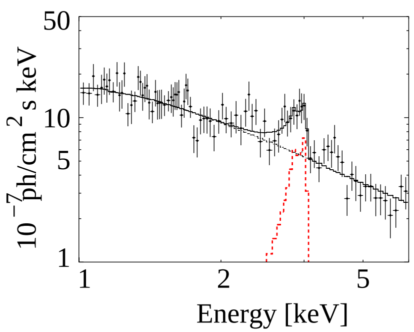

(Comastri, Brusa & Civano, 2004, *Chandra*)
CXO J123716.7+621733 (CDF-N; $z = 1.146$)

Broad Fe Kα lines already present in high-z universe!

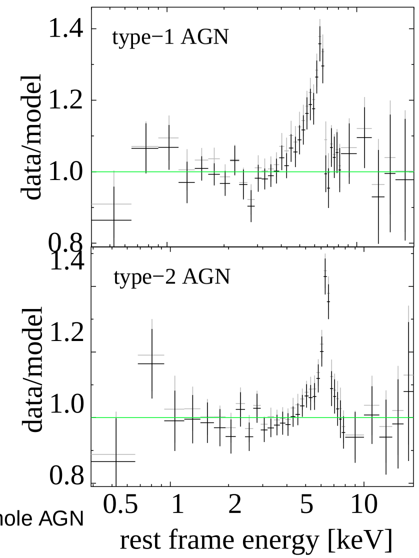

Average Fe line for the Lockman hole AGN (Streblyanska et al., 2005)

3–37

Bianchi, S., Matt, G., Balestra, I., Guainazzi, M., & Perola, G. C., 2004, A&A, 422, 65

Boller, T., Tanaka, Y., Fabian, A., Brandt, W. N., Gallo, L., Anabuki, N., Haba, Y., & Vaughan, S., 2003, MNRAS, 343, L89

Comastri, A., Brusa, M., & Civano, F., 2004, MNRAS, 351, L9

Fabian, A. C., Miniutti, G., Gallo, L., Boller, T., Tanaka, Y., Vaughan, S., & Ross, R. R., 2004, MNRAS, 353, 1071

Fabian, A. C., et al., 2002, MNRAS, 335, L1

Fabian, A. C., et al., 2009, Nature, 459, 540

Guainazzi, M., et al., 1999, A&A, 341, L27

Iwasawa, K., et al., 1996, MNRAS, 282, 1038

Iwasawa, K., Miniutti, G., & Fabian, A. C., 2004, MNRAS, 355, 1073

Jiménez-Bailón, E., Piconcelli, E., Guainazzi, M., Schartel, N., Rodríguez-Pascual, P. M., & Santos-Lleó, M., 2005, A&A, 435, 449

Lee, J. C., Fabian, A. C., Brandt, W. N., Reynolds, C. S., & Iwasawa, K., 1999, MNRAS, 310, 973

Longinotti, A. L., Cappi, M., Nandra, K., Dadina, M., & Pelletrini, S., 2003, A&A, 410, 471

Lubiński, P., & Zdziarski, A. A., 2001, MNRAS, 323, L37

Markoff, S., Nowak, M. A., & Wilms, J., 2005, ApJ, 635, 1203

Martocchia, A., Matt, G., & Karas, V., 2002, A&A, 383, L23

Matt, G., Porquet, D., Bianchi, S., Falocco, S., Maiolino, R., Reeves, J. N., & Zappacosta, L., 2005, A&A, 435, 867

Miniutti, G., & Fabian, A. C., 2004, MNRAS, 349, 1435

Nandra, K., George, I. M., Mushotzky, R. F., Turner, T. J., & Yaqoob, T., 1997, ApJ, 477, 602

Petrucci, P. O., & Henri, G., 1997, A&A, 326, 99

Porquet, D., & Reeves, J. N., 2003, A&A, 408, 119

Reeves, J. N., Turner, M. J. L., Pounds, K. A., O'Brien, P. T., Boller, T., Ferrando, P., Kendziorra, E., & Vercellone, S., 2001, A&A, 365, L134

3–37

Streblyanska, A., Hasinger, G., Finoguenov, A., Barcons, X., Mateos, S., & Fabian, A. C., 2005, A&A, 432, 395

Tanaka, Y., et al., 1995, Nature, 375, 659

Wilms, J., Reynolds, C. S., Begelman, M. C., Reeves, J., Molendi, S., Staubert, R., & Kendziorra, E., 2001, MNRAS, 328, L27